Hierarchical criteria to promote fast and selective a GB precipitation at b grain boundaries in b-metastable Ti-alloys

Tao Liu, Lionel Germain, Julien Teixeira, Elisabeth Aeby-Gautier, Nathalie Gey

Full length article

Hierarchical criteria to promote fast and selective α_{GB} precipitation at β grain boundaries in β-metastable Ti-alloys

Tao Liu [a, b], Lionel Germain [a, b], Julien Teixeira [b, c], Elisabeth Aeby-Gautier [b, c], Nathalie Gey [a, b, *]

[a] Laboratoire d'Etude des Microstructures et de Mécanique des Matériaux, CNRS, Université de Lorraine, 7 rue Félix Savart, METZ F-57073 CEDEX 03, France
[b] Laboratory of Excellence for Design of Alloy Metals for Low-mass Structures ('DAMAS' Labex), University de Lorraine, France
[c] Institut Jean Lamour, CNRS, Université de Lorraine, 2 Allée André Guinier, Campus ARTEM, NANCY F-54000 CEDEX, France

ARTICLE INFO

Keywords:
Titanium
Phase transformation
Grain boundary
Variant selection
Habit plane

ABSTRACT

Early grain boundary (GB) decoration was analyzed in a β-metastable titanium alloy by using electron backscatter imaging and diffraction. More than 1000 GBs were analyzed and classified as 'special' or 'general' GBs: A boundary is called 'special' if it is able to form an α_{GB} layer satisfying the Burgers Orientation Relationship (BOR) with both grains within an angular deviation $\theta_{2\text{-BOR}}$; the others are called 'general' GBs. First, the result gives the probability of a GB to transform early according to a disorientation criterion. 49.5°, 60°/<110> special HAGBs are clearly identified as preferential GBs for early precipitations whereas 60°/<111> special HAGBs behave as general GBs. Second, the probability for transformed GBs to respect the double-BOR variant selection (VS) criterion according to $\theta_{2\text{-BOR}}$ deviation is evaluated. The probability is close to 100% for GBs with $\theta_{2\text{-BOR}}$ up to 10°, random for GBs with $\theta_{2\text{-BOR}}$ over 16°, and decreases progressively but remains higher than random with $\theta_{2\text{-BOR}}$ in between, i.e. an intermediate domain. In addition the habit plane (HP) VS criterion was considered based only on single trace analysis between HP and GB plane (GBP). In most cases, the HP closeness to the GBP was not a relevant VS criterion.

1. Introduction

Large α regions with a single orientation are known to harm the in-service fatigue performance of titanium alloys as they act as fatal crack initiation sites [1–4]. In β-transformed microstructures, these large regions consist of α Widmanstätten colonies (α_{WGB}) growing at each side of the parent β grain boundary (GB). Their single orientation is directly inherited from that of the allotriomorph α layer (α_{GB}) which decorates the parent GB and acts as a precursor. The critical configuration for mechanical properties occurs when this α_{GB} layer results from a variant selection (VS) mechanism at the β GB, favoring common variants between both grains [2,5]. Thus a better control of the in-service properties requires a better understanding of the parameters controlling the orientations of the α_{GB} layer.

Different VS criteria have been proposed in the literature to predict the orientation of α_{GB} precipitates [5,6]. They can be split into two main categories as a function of the number of GB parameters required for the prediction. Some require only the disorientation between the β grains (3-parameters) [5–8] and others need in addition the 3D characteristics of the GB plane (GBP) (5-parameters). For example, 3-parameters criteria consist in selecting the variant that minimizes the deviation to the orientation relationship with both parent grains [6] or only the deviation between close-packed planes involved in the transformation [7–9]. 5-parameters criteria consist in selecting the variant that aligns its habit plane (HP) with the GBP (HP∥GBP) or its close-packed direction in the GBP (CPD∥GBP) [10–12].

In practice, none of them are fully predictive. However important features of the starting microstructure and the transformation conditions are often neglected when the VS frequency for a given criterion is discussed. The fraction of available GBs able to fulfill a given criterion must be quantified and compared to the fraction of transformed GBs. Also, VS analysis requires statistics. Especially, results on the role of the 3D GB character are often limited to few GB configurations as they require time-consuming 3D imaging analysis [10,11]. Moreover, the transformation kinetics is rarely

* Corresponding author.
E-mail address: nathalie.gey@univ-lorraine.fr (N. Gey).

taken into account. Recently Salib et al. considered the relationship between α_{GB} formation kinetics and VS (considering the transformation progress for different undercooling temperatures) [5,13]. They found that VS frequency of α_{GB} layers (for a 3-parameters criterion) decreases with the transformation progress. This implies that α_{GB} VS is favored at the beginning of the transformation [5]. Thus, the earliest stages of the transformation should be considered to establish more predictive VS criteria. To date, published studies consider mostly the end of α precipitation, with no possibility to identify firstly precipitated α_{GB} layers. Moreover, these firstly precipitated α_{GB} are more critical since they emit earlier α_{WGB} colonies. Depending on the thermal treatment applied, these colonies grow in the parent grain to form large single oriented domains.

To identify more predictive VS criteria, the objective of our contribution is to analyze orientation-selective nucleation and growth of α_{GB} layers at the early transformation stage. For this purpose, a short isothermal treatment at 800 °C for 200 s was applied to a Ti-17 sample so that α_{GB} layers had grown only along a limited number of GBs. First, scanning electron microscope (SEM) observations and electron backscatter diffraction (EBSD) analyses were performed to identify β disorientations that favor (or not) fast growth of specific α_{GB} variant. Second, an additional analysis of the EBSD data is proposed to evaluate the relevance of the HP∥GBP criterion in the α_{GB} VS. For this purpose, we have performed an automated β GB trace analysis on the EBSD orientation maps. The GBP traces were compared to the HP traces of the selected variants. This trace analysis between the GBP and HP produces statistical data to discuss the importance of the HP∥GBP VS mechanism. The result of this research may lead to hierarchizing β GB character that promotes fast and selective α_{GB} nucleation and growth. This may help to better evaluate the frequency of critical α_{GB} precursors according to the β microtexture and phase transformation path.

2. Main crystallographic aspects of β→α transformation

2.1. BOR and double-BOR

The β→α transformation in titanium is well known to respect the Burgers Orientation Relationship (BOR) ($\{110\}_\beta \| \{0001\}_\alpha$ and $<1\bar{1}1>_\beta \| <11\bar{2}0>_\alpha$) in which each β grain can generate a maximum of 12 α variants.

At a β GB, the α_{GB} precipitation has been reported to satisfy BOR with both grains [14]. This phenomenon is here called double-BOR VS (abbreviated as 2-BOR in the following subscripts). However, it requires special disorientations between the parent β grains as reported in Table 1. The list is easily obtained by calculating all possible disorientations between the potential parents of a given variant as explained in Ref. [14].

Type I is a low angle GB (LAGB), while the others are high angle GBs (HAGBs). Table 1 also shows that Type III and IV β GBs have multiple common variants because of their special disorientation configurations. Table 1 disregards the trivial configuration of low disoriented β grains for which 12 variants would be common.

2.2. Habit plane

The HP is another important crystallographic aspect of phase transformation. In titanium alloys, several studies report a $\{334\}_\beta$ HP for the β→α′ martensitic transformation [15] and a HP near $\{334\}_\beta$ in diffusional precipitation of intragranular α [16,17]. Moreover, this result is supported by different calculations of the HP taking into account the transformation strain energy. Considering either a thin infinite plate [18,19] or a phase field model [20], the HP for α is approximately $\{334\}_\beta$. Slight differences may be obtained in association with different transformation strain tensor and any possible plastic accommodation during the transformation [21]. Table 2 shows the 12 crystallographic equivalent BORs with the close-packed planes $\{110\}_\beta$ and directions $<111>_\beta$. The corresponding {334} HPs are listed in the right column. The HP has also been proposed to play a role in the selection of the α layer forming at a β GB: the α_{GB} is considered to preferentially form if its HP is close to the prior β GBP [10].

3. Experimental

3.1. Materials

The Ti-17 β-metastable alloy was selected to study the early stage of β→α GB transformation. With a chemical composition (wt.%) of (Al:5%, Cr:4%, Mo:4%, Sn:2%, Zr:2%, O_2:1200 ppm, Ti in balance), the β transus temperature (T_β) is 880 °C. A cylindrical sample was submitted to a controlled thermal treatment. It was first solution treated in the β phase field at 920 °C for 30 min. After solution treatment, the β grains were equiaxed with an average diameter of 200 μm. The macroscopic β texture was close to random. However, the spatial orientation distribution of the β grains (microtexture) was not random. The fraction of LAGBs (characterized by a disorientation angle below 15°) was of 20% which is much higher than the 2.3% expected in a random cubic poly-crystal [22]. When only HAGBs were considered, the distribution was close to random.

After the dwell at 920 °C, the specimen was rapidly helium quenched to the transformation temperature T of 800 °C and isothermally treated for 200 s. For the considered undercooling (T_β-T) of 80 °C, the transformation is known to start at β triple junctions. Then the GBs are decorated by α_{GB} and finally α_{WGB} Widmanstätten colonies are emitted from those α_{GB} (see the Ti-17 TTT diagram published in Ref. [23]). Moreover, the isothermal transformation kinetics is slow enough to control the decoration proportion of β GBs. It was estimated to be 12% after 200 s, 65% after 700 s and 94% after 6 h isothermal holding [24]. Thus a 200s holding time was selected to restrict the transformation to the firstly formed α_{GB}.

3.2. Imaging and EBSD data acquisition

The Ti-17 sample was mechanically ground with SiC papers and then electrolytically polished with a solution containing methanol and perchloric acid. The α_{GB} layers were imaged with the backscatter electron detector (BSE-D) under the ZEISS Auriga Focus Ion Beam Scanning Electron Microscope (FIB-SEM). Crystallographic orientation maps were acquired with the Bruker QUANTAX EBSD acquisition system. Two mapping strategies were decided for EBSD data acquisition:

Strategy A: Large-area maps were performed in multi-mapping mode. The total scanned area of 8 mm × 0.8 mm (step size: 1 μm) covered a large number of β GBs (1129 GBs). In addition, the EBSD scanned β GBs were further imaged in BSE mode to identify the presence of α_{GB} precipitation.

Strategy B: 74 transformed GBs identified on the above area were finely scanned by EBSD with a smaller step size of 0.25 μm for further VS analysis.

3.3. Automated EBSD data analysis

The EBSD maps were processed with our home-made software called DECRYPT (Direct Evaluation of CRYstallographic Phase

Table 1
Four types of β disorientations allowing the β grains to strictly share common variants.

Special β GB type	β disorientation	Number of common variants
I	10.5°/<110>	1
II	49.5°/<110>	1
III	60°/<110>	**2**
IV	60°/<111> (equivalent to 70.5°/<110>)	**3**

Transformation). This software is dedicated to analyzing the orientation data inherited by OR-based phase transformations. Two main processing routes available in the software were applied: (1) Quantification of GB transformation with respect to the double-BOR criterion and (2) Analysis of parent GBP traces versus HP traces.

3.3.1. Quantification of GB transformation with respect to the double-BOR criterion

DECRYPT was applied first to quantify the fraction of β GBs able to share close-oriented α_{GB} variants (minimizing the BOR deviation with both grains) and second to quantify the GBs preferentially decorated by these close-oriented α_{GB} variants.

(1) The β GBs able to share close α_{GB} variants were identified on the EBSD maps obtained with Strategy A. DECRYPT detects the β grains and GBs with a user-defined critical disorientation angle (3° in the present study). At each β GB, all theoretical pairs, $\alpha_i^{th-\beta1}/\alpha_i^{th-\beta2}$, of α variants inherited respectively from β1 and β2 are considered. The disorientation angles between all pairs, $\{\theta(\alpha_i^{th-\beta1}/\alpha_j^{th-\beta2})\}_{i=1,12;j=1,12}$, are calculated. The GB satisfies the so-called 'double-BOR condition at $\theta_{2\text{-BOR}}$' if at least one variant pair is disoriented below the user-defined threshold angle ($\theta_{2\text{-BOR}}$). If it respects this condition it is defined as a 'special GB' and if not it is defined as 'general GB'. DECRYPT exports for all GBs: (a) the GB length for each detected GB, (b) the theoretical variant pair $(\alpha_i^{th-\beta1}/\alpha_j^{th-\beta2})$ with the smallest disorientation angle $\theta(\alpha_i^{th-\beta1}/\alpha_j^{th-\beta2})<\theta_{2\text{-BOR}}$ (multiple solutions if available) and (c) the corresponding disorientation angle $\theta(\alpha_i^{th-\beta1}/\alpha_j^{th-\beta2})$.

(2) For the decorated boundaries, the orientation of the α_{GB} layer was further measured by EBSD with Strategy B. DECRYPT determines if the α_{GB} variant was preferentially selected to minimize BOR with both β grains, i.e., if it respects the double-BOR VS criterion.

Table 2
12 crystallographic equivalent ORs from β to α phase transformation and corresponding HPs.

No. of variant	OR	Habit Plane
α_1^{th}	$(110)[1\bar{1}1]$	$(3\bar{3}\bar{4})$
α_2^{th}	$(110)[\bar{1}11]$	$(\bar{3}\bar{3}4)$
α_3^{th}	$(1\bar{1}0)[111]$	$(33\bar{4})$
α_4^{th}	$(1\bar{1}0)[11\bar{1}]$	(334)
α_5^{th}	$(10\bar{1})[111]$	$(3\bar{4}3)$
α_6^{th}	$(10\bar{1})[1\bar{1}1]$	(343)
α_7^{th}	$(101)[\bar{1}11]$	$(34\bar{3})$
α_8^{th}	$(101)[11\bar{1}]$	$(3\bar{4}\bar{3})$
α_9^{th}	$(011)[11\bar{1}]$	$(\bar{4}\bar{3}3)$
α_{10}^{th}	$(011)[1\bar{1}1]$	$(43\bar{3})$
α_{11}^{th}	$(01\bar{1})[\bar{1}11]$	(433)
α_{12}^{th}	$(01\bar{1})[111]$	$(\bar{4}\bar{3}\bar{3})$

For this purpose, the α_{GB} orientation is related to the closest theoretical $\alpha^{th-\beta1}$ variants and $\alpha^{th-\beta2}$ variants. θ_1 and θ_2 are the disorientation angles between the α_{GB} orientation and each β1-and β2-closest theoretical variants. These angles quantify the angular deviations of the α_{GB} layer from a strict BOR, respectively with β1 and β2 grain. The β grain with the smallest deviation is called the BOR grain. Furthermore, the variant pair $(\alpha_i^{th-\beta1}/\alpha_j^{th-\beta2})$ minimizing BOR is known from step (1) as well as the corresponding disorientation angles $\theta(\alpha_i^{th-\beta1}/\alpha_j^{th-\beta2})$. The VS criterion is satisfied at $\theta_{2\text{-BOR}}$ if the β1-and β2-closest variants to the α_{GB} orientation corresponds to this variant pair $(\alpha_i^{th-\beta1}/\alpha_j^{th-\beta2})$ and consequently θ_1(resp. θ_2) $<\theta(\alpha_i^{th-\beta1}/\alpha_j^{th-\beta2})<\theta_{2\text{-BOR}}$.

However, two weak points of the double-BOR VS criterion need to be mentioned. First, it cannot predict the BOR grain at the considered β GB. Second, it cannot discriminate between multiple variant pairs for Type III and IV GBs. As observed in our sample, a GB disoriented by 54.9° around $[\bar{3}04]$ was close to Type III GB. Two variant pairs output by DECRYPT software satisfy the double-BOR condition at $\theta_{2\text{-BOR}} = 6.9°$: Pair I - $\alpha_{12}^{th-\beta1}/\alpha_6^{th-\beta2}$; Pair II - $\alpha_{11}^{th-\beta1}/\alpha_5^{th-\beta2}$. The observed α_{GB} variant was actually close to $\alpha_{12}^{th-\beta1}$. For such configurations, we have considered that the VS criterion was satisfied, even if it was not possible to discriminate both solutions.

3.3.2. Analysis of parent GBP traces versus HP traces

DECRYPT includes automated trace analysis on an EBSD map to compare the GBP traces with the HP traces. Our purpose is to analyze the relevance of the so-called HP criterion: the α_{GB} variant preferentially selected has its HP normal forming the smallest angle off the GBP normal. In this context, we have applied a trace analysis on a single section. This enables only to identify the transformed GBs for which the HP criterion can be excluded.

First, the normal to each GB trace of the EBSD map is obtained by calculating the first order moment of the grain map as proposed by Lieberman et al. [25]. Then the angles between the GBP trace and the 12 HP traces, $\{\theta_{HP}\}_{i=1,12}$, are calculated for each grain forming the GB. The variants with θ_{HP} below a user-defined threshold ($\theta_{HP\text{-limit}}$) are stored. If no HP trace lies close to the GBP trace (i.e. all θ_{HPi} are higher than $\theta_{HP\text{-limit}}$), the GB can never respect the HP∥GBP criterion. This analysis was applied to the EBSD maps acquired with Strategy A. $\theta_{HP\text{-limit}}$ was defined at 10°. Only 15% of the GBs were identified as unable to respect the HP∥GBP criterion. This is not surprising. Indeed, GBs identified as having an HP-GBP trace deviating by less than 10° are very numerous but they have much larger angles between both planes in 3D. So this approach is not selective but definitely includes a lot of boundaries far from being able to have a small deviation between the GBP and a potential HP.

The approach becomes more relevant when the α_{GB} variant (and its HP) formed at the GB is considered for further VS analysis of the maps acquired with Strategy B. From a practical point of view, the BOR grain and the selected variant are known for each α_{GB} layer. For this BOR grain, the HP traces of the 12 variants are compared to the GBP trace (DECRYPT exports the variants with $\theta_{HP}<\theta_{HP\text{-limit}}$ (10°), they are called potential HP-variants). If the α_{GB} variant does not belong to these potential HP-variants (i.e. its HP trace is not aligned with the GBP trace), the HP criterion is not respected at this GB.

4. Results

After 200 s holding time at 800 °C, the β→α phase transformation occurred along the β GBs as expected. 16.2% (in length) of the GBs had α_{GB} precipitates. This value was obtained over the EBSD maps acquired with strategy A (1129 GBs in total) by combining the GB list exported by DECRYPT software with the analysis of the BSE images. It refines the previous amount of 12% obtained in the same

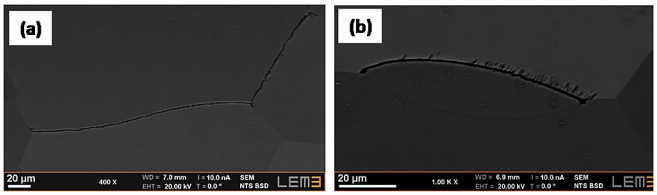

Fig. 1. GBs fully decorated by (a) an α_{GB} layer at the early stage of transformation and (b) early emission of α Widmanstätten colonies.

condition in Ref. [5].

Moreover, the transformation occurred only on a limited number of GBs that were almost fully decorated by a 1 µm thick α_{GB} layer having essentially a single orientation (Fig. 1a). Those β GBs fully decorated at the early stage of transformation were preferential sites for nucleation and growth of α_{GB} layers. It shall be stressed that Salib et al. pointed out that early α_{GB} precipitation is related to early α_{WGB} emission which leads to larger colonies, as seen in Fig. 1b [5].

These early transformed GBs were further analyzed to determine what influences their preferential precipitation. For this purpose, all 1129 GBs were analyzed to identify 'special' versus 'general' GBs[1] and to quantify their transformation frequency at the early stage of transformation (for each category, LA- and HA-GBs were distinguished).

4.1. Transformation frequency of special GBs

Special β GBs able to strictly share common variants were quantified on the EBSD maps acquired with Strategy A. $\theta_{2\text{-BOR}} = 3°$ was first applied to account for experimental precision. The results are summarized in Table 3. The length fraction of special β GBs to the total GBs was found to be only 2.6% (GB fraction in number: 32 over the 1129). Most of them (26 over the 32) were of Type I, meaning LAGBs disoriented by 10.5°/<110>. Additional BSE images show that these Type I GBs had a very low transformation frequency (2.1% in length fraction or 3/26 in number). Among the other three types of special GBs belonging to HAGBs, Type II and III were almost fully transformed whereas the single Type IV GB inventoried was not transformed at all. However, the number of strict special GBs is too low to deduce a reliable transformation frequency and the $\theta_{2\text{-BOR}}$ angle was increased to further interpret these results.

The fraction of GBs considered as 'special' with increasing $\theta_{2\text{-BOR}}$ is plotted in Fig. 2. The reasonable $\theta_{2\text{-BOR}}$ threshold values were set to identify special GBs. With $\theta_{2\text{-BOR}}$ increasing from 3° to 6°, the fraction of special GBs increases rapidly. However, the main contribution to this increase is ascribed to Type I - LAGBs. Actually, Type I-LAGBs extend over the high fraction of LAGBs present in the Ti-17 sample. Special HAGBs (i.e. Type II, III and IV together) are expected to transform with a high frequency but their fraction increases little. At $\theta_{2\text{-BOR}} = 6°$, Type I LAGBs account for 18% of all GBs, and special HAGBs only for 5% (Type II: 1.9%, Type III: 1.7%, Type IV: 1.4%). Finally a threshold $\theta_{2\text{-BOR}} = 10°$ gives a fraction of special HAGBs of 15% which is close to the fraction of transformed boundaries in our sample. One can notice that Type IV contributes the least to this 15% (Type II: 6.8%, Type III: 6.1%, Type IV: 2.1%).

In the following, special GBs were identified by increasing $\theta_{2\text{-BOR}}$ up to 6° and 10° and their transformation frequency quantified. Each type of special GBs is distinguished in Fig. 3. It can be compared with the average transformation frequency of all LAGBs and HAGBs found in our sample: 4.1% for all LAGBs and 19.2% for all HAGBs. Three main tendencies were found for strict special GBs:

(1) The numerous Type I-LAGBs were found to have a very low transformation frequency despite their capacity to share close variants. It was of 5.6% for $\theta_{2\text{-BOR}} = 3°$ (26 GBs), 2.8% for $\theta_{2\text{-BOR}} = 6°$ (206 GBs) and 4.3% for $\theta_{2\text{-BOR}} = 10°$ (293 GBs), i.e. it was slightly changed at different $\theta_{2\text{-BOR}}$. The fractions are close to the average transformation frequency of all LAGBs. So Type I GBs transform at a similar rate as any LAGB.
(2) Type II and III-HAGBs were confirmed to transform with a high frequency at the early stage. It was of 90% for $\theta_{2\text{-BOR}} = 3°$ (only 5 GBs) and remained high with increasing $\theta_{2\text{-BOR}}$: 73% for $\theta_{2\text{-BOR}} = 6°$ (35 GBs) and 46.5% for $\theta_{2\text{-BOR}} = 10°$ (132 GBs). This frequency is much higher than the average value of all HAGBs.
(3) Type IV HAGBs had a significantly lower transformation frequency than Type II and III. It was of 0% for $\theta_{2\text{-BOR}}<3°$ (only1 GB), around 22% for $\theta_{2\text{-BOR}}<6°$ (15 GBs) and 24% for $\theta_{2\text{-BOR}}<10°$ (22 GBs). This frequency is close to the average value of all HAGBs. Type IV GBs transform like any other HAGBs.

This analysis shows that only Type II and III special GBs are clearly identified as having a significant advantage for early decoration by a common α_{GB} variant (as described in Section 4.3). As a consequence, they are critical GBs for the development of large and single oriented α_{WGB} colonies.

4.2. Contribution of general GBs to the transformation

Even if special GBs have a high transformation frequency, our result shows that the major fraction of transformed boundaries were actually general HAGBs. This is evidenced in Fig. 4 where all transformed boundaries are classified into 6 categories: special GBs of Type I to IV and general LA-/HA-GBs (special/general GBs are discriminated by applying $\theta_{2\text{-BOR}}$ of 6° and 10°). General HAGBs account for 80.7% of the transformed boundaries when special GBs are identified at $\theta_{2\text{-BOR}} = 6°$, and 56.8% at $\theta_{2\text{-BOR}} = 10°$. Special HAGBs and especially Type II and III are clearly observed to transform with a high frequency at the early stage of transformation. However, strict Type II and III are rare in our sample. With increasing the tolerance of the double-BOR condition, their transformation frequency drops (Figs. 2 and 3). This may explain why these special GBs represent a significant but not major fraction of the transformed GBs at the early stage of transformation.

We have questioned if among the general HAGBs, some had a transformation advantage with respect to two disorientation criteria. The deviation from the double-BOR condition was the first disorientation criterion considered. Fig. 5a plots the fraction of transformed HAGBs as a function of $\theta_{2\text{-BOR}}$ and compares it with the average values of either for all HAGBs (19.2%, bold dotted line) or all general HAGBs (15%, thin dotted line). Most of general HAGBs ($\theta_{2\text{-BOR}}>10°$) do not have a transformation rate significantly higher than the average (15%). The maximum is found for GBs with $\theta_{2\text{-BOR}}$ between 22° and 24°. This peak corresponds mostly to GBs with a disorientation angle of 30° which are about 20° off Type I and II.

To better highlight this specific behavior of 30° disoriented GBs, the transformation frequency of general HAGBs is plotted according to their disorientation angle in Fig. 5b. It clearly confirms that their transformation rate is significantly higher (35%) than the average (15%). A tentative to relate this phenomenon to the disorientation axes of those GBs revealed no clear trend. Actually more statistics would be needed to explore the disorientation space of the GBs.

In addition, Fig. 5a points out an interesting aspect of the 10°

[1] A boundary is defined as 'special' if it is able to share common variants at $\theta_{2\text{-BOR}}$. The other boundaries are called 'general' GBs.

Table 3
Fraction of strict special GBs identified in the Ti-17 sample and their transformation frequency.

	Fraction of special GBs ($\theta_{2\text{-BOR}}<3°$)	Transformed fraction per type of special GBs			
		Type I (10.5°/<110>)	Type II (49.5°/<110>)	Type III (60°/<110>)	Type IV (60°/<111>)
in number	32/1129 GBs	3/26 GBs	3/4 GBs	1/1 GB	0/1 GB
in length	2.6%	2.1%	88%	100%	0%

threshold used to discriminate the special from the general GBs. As discussed, it is observed in Fig. 5a that the transformation frequency of special GBs decreases with increasing $\theta_{2\text{-BOR}}$ from 0° to 10° but it remains always higher than the average values. Over 10° this is no longer the case. This indicates that the threshold value of 10° to discriminate special GBs makes sense.

4.3. α_{GB} VS: relevance of the double-BOR criterion

74 transformed GBs were finely EBSD-mapped with Strategy B as detailed in Section 3.2. Our purpose was to test if the double-BOR criterion is able to predict the observed α_{GB} variants. Fig. 6 shows an example of special GB for which the double-BOR criterion is predictive. The β1 and β2 were disoriented by 47.4°/[$\bar{4}$30] (close to a Type II GB). They can transform to a pair of theoretical variants ($\alpha_3^{th-\beta1}/\alpha_3^{th-\beta2}$) disoriented by $\theta(\alpha_3^{th-\beta1}/\alpha_3^{th-\beta2}) = 5.9°$. The α_{GB} variant observed at this GB was close to these predicted variants, so that it minimized BOR with both β grains. The arrow-indicated pole

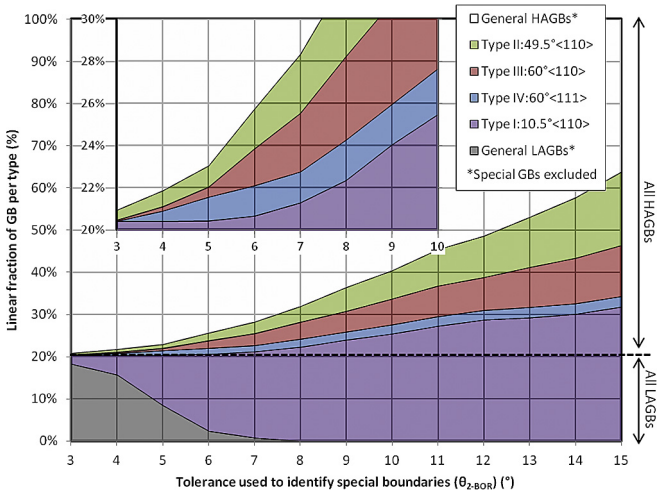

Fig. 2. Fraction of special β boundaries in the Ti-17 sample as a function of $\theta_{2\text{-BOR}}$ (inset a close-up for low $\theta_{2\text{-BOR}}$). Notice that for $\theta_{2\text{-BOR}}>5.25°$, the disorientation space of each special GB overlaps; the GB is then assigned to the closest type. The rest of the GBs were classified as LAGBs and HAGBs according to the classical 15° disorientation angle.

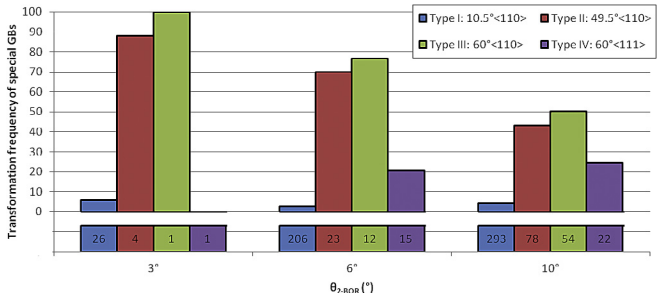

Fig. 3. Cumulative transformation frequency of special GB types for $\theta_{2\text{-BOR}}< 3°, 6°, 10°$ (the number of GBs is indicated below each histogram).

on the superimposed β/α pole figures confirms the plane and direction alignment. The β2 grain was the BOR grain ($\theta_2 = 0.9°$) and β1 the non-BOR grain ($\theta_1 = 5.5°$).

This analysis was applied to all GBs. 41 out of the 74 analyzed GBs are identified as special GBs at $\theta_{2\text{-BOR}} = 10°$: 2 Type I, 26 Type II, 10 Type III and 3 Type IV. This distribution of transformed GBs agrees with Fig. 3, so as further to suggest that the analyzed GBs were representative of the general tendency of the sample. We found that all 41 special GBs respect the double-BOR VS criterion, i.e. the selected α_{GB} variant was the one that minimizes the BOR deviation with both β grains. This indicates a 100% prediction accuracy of the double-BOR criterion for special GBs identified up to $\theta_{2\text{-BOR}} = 10°$.

Fig. 7 shows the influence of increasing $\theta_{2\text{-BOR}}$ deviation (up to its maximum value of 30°) on the prediction accuracy. The result is compared to the level of random occurrence of this criterion (10.3%[2]). Any $\theta_{2\text{-BOR}}$ increment beyond 10° results in a drop of the prediction accuracy. Moreover, the prediction is at the random level for $\theta_{2\text{-BOR}}$ greater than 16°. Among the 74 transformed GBs, 24 belong to this category. They were all decorated at the early stage of the transformation with a unique α_{GB} variant but the double-BOR criterion is only predictive for 10%. The α_{GB} layer of these GBs was well aligned in BOR with one β grain but deviated from the BOR with the other grain: much higher than their $\theta_{2\text{-BOR}}$ (>19°).

As a result, our research comes to the law that defines the probability to respect the double-BOR criterion according to their $\theta_{2\text{-BOR}}$ deviation: (1) up to $\theta_{2\text{-BOR}}$ of 10°, the double-BOR criterion is 100% respected; (2) over 16°, this criterion is insignificant; (3) in between we found an intermediate domain for which the VS frequency decreases progressively but remains higher than random. This intermediate domain is defined by rather low statistics and shall be refined in the future.

4.4. α_{GB} VS: relevance of HP closeness to GBP

As explained in Section 3.3.2, a single trace analysis was applied to the transformed GBs to identify the GBs for which the HP criterion can be excluded. The methodology is first illustrated on four GBs. Then the result over the 74 transformed GBs is summarized to discuss the relevance of the HP criterion. At this step one has to highlight the complex α_{GB} morphology observed at some GBs. Indeed, α_{GB} layers did not always 'wet' the straight or curved GBs (Figs. 8a and 9a) but 22% of the GBs exhibited a zig-zag morphology (Figs. 8d and 9d). This morphology has been observed in the literature and results from the branching of the α_{GB} layer. This mechanism destabilizes the GB that finally adopts the zig-zag shape, as suggested by Sharma [26]. The four selected GBs (referred to as A, B, C, D) presented an α_{GB} layer with either a planar or a zig-zag morphology. They were general GBs and therefore not able to satisfy the double-BOR condition below 10°. The determination of the GBP trace of a zig-zag GB is somehow questionable. For those

[2] This value takes into account multiple solutions for GBs close to Type III and IV. The different types of GBs observed in our Ti-17 sample are quantified at the maximum $\theta_{2\text{-BOR}}$: 45% of Type I, 36% of Type II, 15% of Type III and 4% of Type IV).

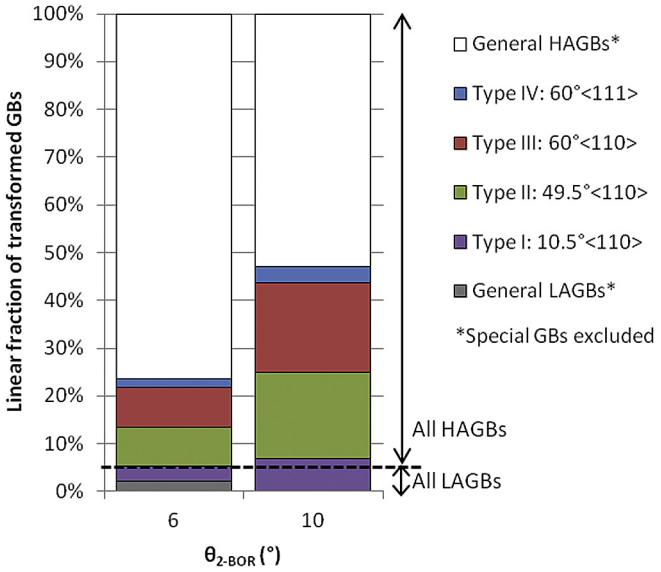

Fig. 4. Classification of the transformed GBs in different GB types (general VS special). 100% represents the 16.2% of boundaries decorated by an α_{GB} precipitate.

GBs, we considered two possible traces to describe these zig-zag configurations (referred to as the 1st and 2nd GBP trace).

The results for the BOR grains of each GB are given in Figs. 8 and 9, including the BSE images of the GBs (a,d), the typical figures output by DECRYPT for the trace analysis (c,f) and the stereographic projection of the corresponding HPs with PAN software [27]. In

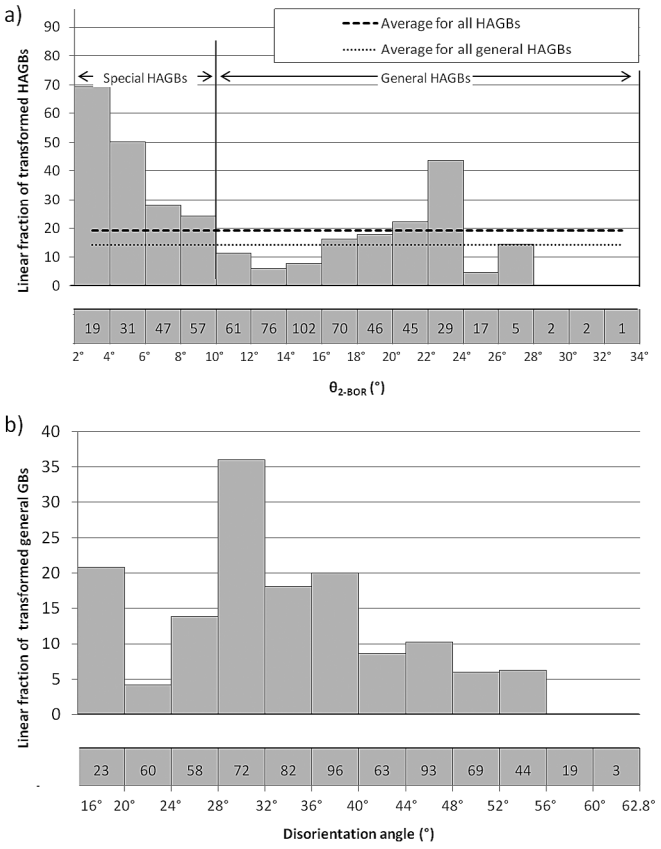

Fig. 5. a) Linear fraction of transformed HAGBs as a function of $\theta_{2\text{-BOR}}$, b) Linear fraction of general GBs as a function of disorientation angle. Data is presented per bin; the amount of data per point is indicated below the histogram.

Figs. 8 and 9 (c,f), the 12 potential variants are discriminated by the attached color code and the star in the corner of each figure represents the normal to the related HP traces. At the GB, the computed GB normal is plotted only for variants with θ_{HP} (angle between the GBP trace and the HP trace) below the threshold value of 10°. The normal has the color of the variant with the closest HP trace to the GBP trace. Moreover, the length of the plotted normal is inversely proportional to θ_{HP}, i.e. the higher the length, the better the fit between the HP and the GBP traces.

Fig. 8 shows the transformed GB A and B for which our approach excludes the role of the HP in the VS. The GB A is rather planar as seen in Fig. 8a. The α_{GB} layer was in BOR with β2 and was close to variant $\alpha_3^{th-\beta2}$. No variant was output by DECRYPT for the BOR grain β2 as displayed in Fig. 8b. For a better view, the 12 H PP traces of β2 were compared with the GBP trace on a pole figure plotted with the PAN software in Fig. 8c: all HP traces of the 12 variants were actually far off the GBP trace. In this case, the HP of the observed variant $\alpha_3^{th-\beta2}$ (colored in green in Fig. 8c) is not close to the GBP ($\theta_{HP} = 28°$).

Fig. 8d shows the GB B with a complex zig-zag morphology. Three potential HP variants are output by DECRYPT for the BOR grain β2: $\alpha_9^{th-\beta2}$, $\alpha_5^{th-\beta2}$ and $\alpha_2^{th-\beta2}$, as displayed in Fig. 8e. All three variants are near the 1st GBP trace and none near the 2nd GBP trace, as plotted in Fig. 8e and f. However, the observed variant is $\alpha_{12}^{th-\beta2}$(colored in green in Fig. 8f) and its HP is not close to the GBP ($\theta_{HP} = 32°$).

Fig. 9 shows the transformed GB C and D for which our approach cannot exclude the role of the HP in the VS. Fig. 9a shows the planar GB C. Three potential HP variants are output by DECRYPT for the BOR grain β2: $\alpha_7^{th-\beta2}$, $\alpha_6^{th-\beta2}$ and $\alpha_4^{th-\beta2}$, as displayed in Fig. 9b. The HP trace of all three variants is close to the GBP trace, as evidenced by the HP and GBP trace comparison in Fig. 9c. The α_{GB} variant observed at this GB was actually $\alpha_7^{th-\beta2}$ (colored in green in Fig. 9c).

Fig. 9d shows the zig-zag GB D. Four variants are output by DECRYPT for the BOR grain β2: $\alpha_7^{th-\beta2}$, $\alpha_3^{th-\beta2}$, $\alpha_6^{th-\beta2}$ and $\alpha_{10}^{th-\beta2}$, as displayed in Fig. 9e. All four variants have an HP trace near the 1st GBP trace and none near the 2nd GBP trace, as shown in Fig. 9f. The observed α_{GB}, $\alpha_3^{th-\beta2}$ (colored in green in Fig. 9f), was among the output HP variants. Additional 3D is required to conclude for both example C and D.

The HP criterion was then tested on the 27 transformed GBs where the double-BOR criterion was not respected. 16 GB ss had no consistency between the observed α_{GB} variant and the predicted HP variants. So, 59.3% of these GBs did not respect the HP criterion. 11 GB ss need to be further analyzed in 3D. The HP criterion was tested over the 47 GBs transformed with an α_{GB} layer respecting the double-BOR criterion (41 have $\theta_{2\text{-BOR}} < 10°$ and 6 have $10° < \theta_{2\text{-BOR}} < 16°$). The purpose was to evaluate if the HP criterion could be an additional criterion able to predict the BOR grain or discriminate between multiple double-BOR variants. The result indicates that for 31 GBs (66%), the observed α_{GB} variant had its HP trace more than 10° deviated from the GBP trace (the other 16 GBs needs to be analyzed in 3D to draw a conclusion). In most cases, the selected double-BOR variant does not in addition minimize its HP closeness to the GBP.

So, the trace analysis allows the HP criterion to be excluded for a large majority of transformed GBs. It suggests that the HP closeness to the GBP is not a relevant criterion to predict the selected variant in most cases.

5. Discussion

5.1. GB transformation frequency

Our result confirms that the α_{GB} layers precipitate on HAGBs

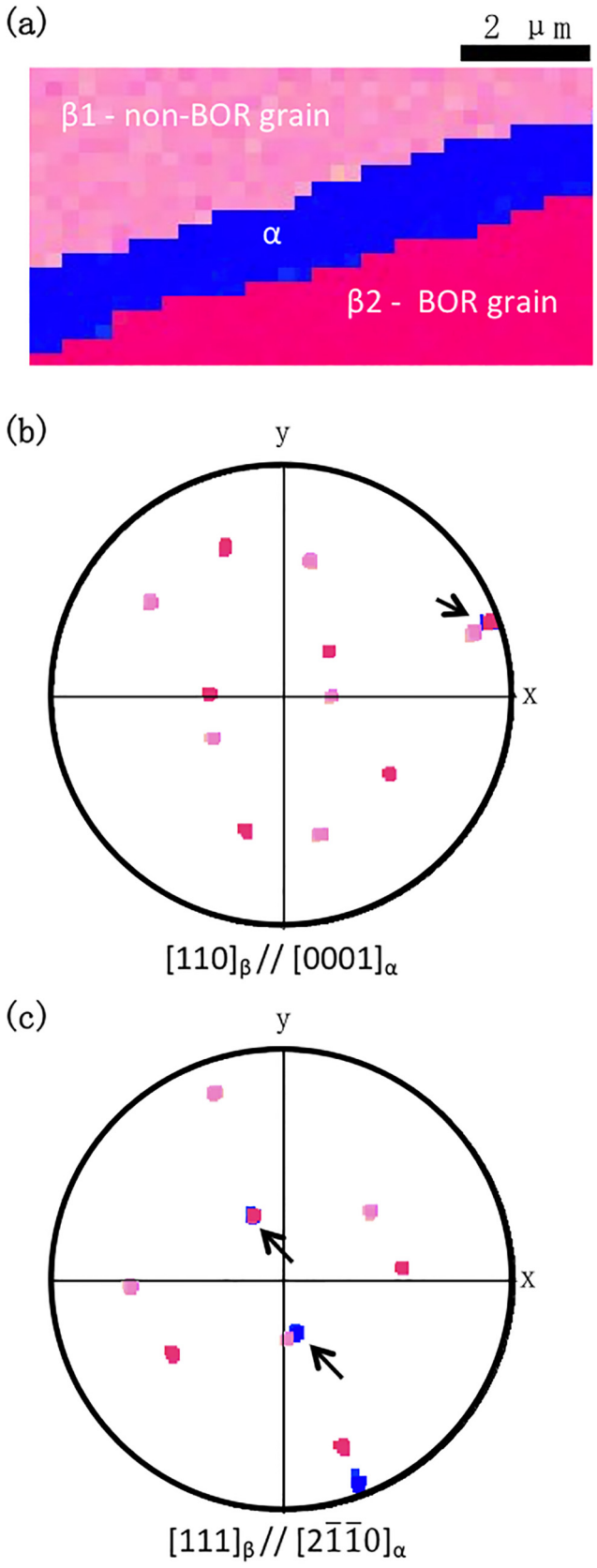

Fig. 6. A transformed GB satisfying the double-BOR criteria (with a deviation of 5.9°): (a) EBSD map showing β1 and β2 grains colored in light and dark pink and α_{GB} layer in blue (The BOR grain and non-BOR grain are indicated); (b) Superimposed $\{110\}_{\beta1/\beta2}$ and $\{0001\}_{\alpha GB}$ pole projections (the arrow indicates the 3 overlapping poles according to the double-BOR criterion); (c) Superimposed $<111>_{\beta1/\beta2}$ and $<2\bar{1}\bar{1}\ 0>_{\alpha GB}$ pole projections (the two arrows indicate the alignment of $\beta1/\alpha_{GB}/\beta2$ close-packed directions). (For interpretation of the references to colour in this figure legend, the reader is referred to the web version of this article).

with a much higher frequency than on LAGBs at the early stage of transformation. Indeed, 19.2% of all HAGBs were almost fully transformed against only 4.1% of LAGBs in the Ti-17 sample. The same conclusion is evidenced by analyzing the 16.2% transformed GBs: among them 94.8% accounted for HAGBs (Fig. 4). This is consistent with previous results in the literature [8,28] which also pointed out that the LAGBs are only partially decorated or not decorated at all, even with higher undercooling temperature and with longer isothermal treatments. HAGBs are clearly more efficient nucleation sites than LAGBs for fast growth of a unique α_{GB} layer over the whole GB. It can be noticed that Type I LAGBs (10.5°/<110>) able to share close α_{GB} variants have no specific advantage for early transformation. In fact, HAGBs are regions of severe localized disorder and are classically identified as high energy boundaries. This explains their advantage for early transformation.

The present study offers clear evidence that special HAGBs (the two neighboring grains able to share close α_{GB} variants) transform with a much higher frequency than general boundaries (Fig. 3). Our home-made software 'DECRYPT' was a key tool to obtain statistical data in this framework. The special boundaries (see Table 1) were identified automatically on EBSD maps by taking a user-defined tolerance $\theta_{2\text{-BOR}}$ into account. The result shows that the transformation frequency of special HAGBs is around 70% for small $\theta_{2\text{-BOR}} = 6°$, which is significantly higher than the average transformation frequency of HAGBs (19.2%) (Fig. 5a). It decreases with increasing $\theta_{2\text{-BOR}}$ values. However, from $\theta_{2\text{-BOR}} = 6°$ to $\theta_{2\text{-BOR}} = 10°$ the transformation frequency remains higher than the average values of HAGBs and beyond 10°, this is no longer the case. This highlights that special HAGBs with a $\theta_{2\text{-BOR}}$ deviation up to 10° are preferential sites for fast nucleation and growth of α_{GB} layers.

The major finding is the important differences in transformation frequency observed according to the type of special HAGBs. Type II and III (49.5°, 60°/<110>) have a very high transformation frequency, close to 100% for low $\theta_{2\text{-BOR}}$ deviations (Fig. 3). However, it must be highlighted that strict Type II and III are rare in a random cubic poly-crystal and their transformation frequency drops by increasing the $\theta_{2\text{-BOR}}$ tolerance (Figs. 2 and 3). Consequently, these special GBs represent a significant but not major fraction of the transformed GBs at the early stage of transformation (Fig. 4). Unexpectedly, Type IV GBs (60°/<111>) have a transformation frequency close to that of general HAGBs. In fact, Type IV GBs are Σ3 boundaries in cubic materials and may have a lower energy in β Ti-alloys. This lower energy may explain their delay for early precipitation.

We conclude that the GB energy is the first order parameter to overcome the nucleation barrier for further growth of an α_{GB} layer along the GB. This makes low energy configurations, e.g. like LAGBs or Σ3, the less energetically favorable nucleation and growth sites for α_{GB} transformation. The link between GB character and energy is more complex. It is admitted that the energy of a GB depends not only on the lattice disorientation or lattice coincidence but also on the GBP [29]. Unfortunately, the relevant literature for body-centered cubic material is rare in comparison to face-centered cubic materials.

The capability of special high energy GBs to share a common variant to both grains is the second order parameter for fast α_{GB} nucleation and growth. As discussed in the next section, these GBs are preferentially decorated by this common variant to build low energy $\beta/\alpha_{GB}/\beta$ interfaces, respecting at best BOR with both β grains. Consequently these GBs may benefit from a favorable

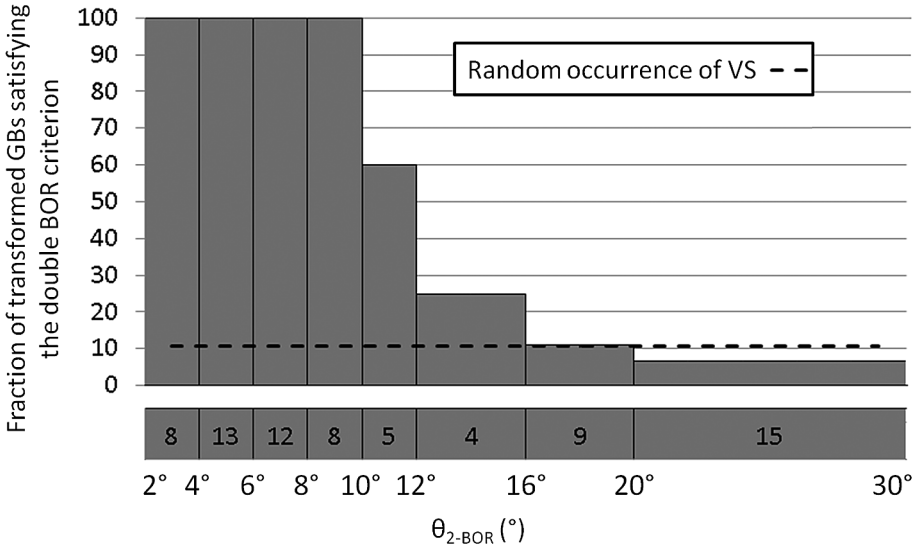

Fig. 7. Fraction of boundaries where the selected variant minimizes the BOR deviation from both β grains. The number of observed boundaries is indicated below each class.

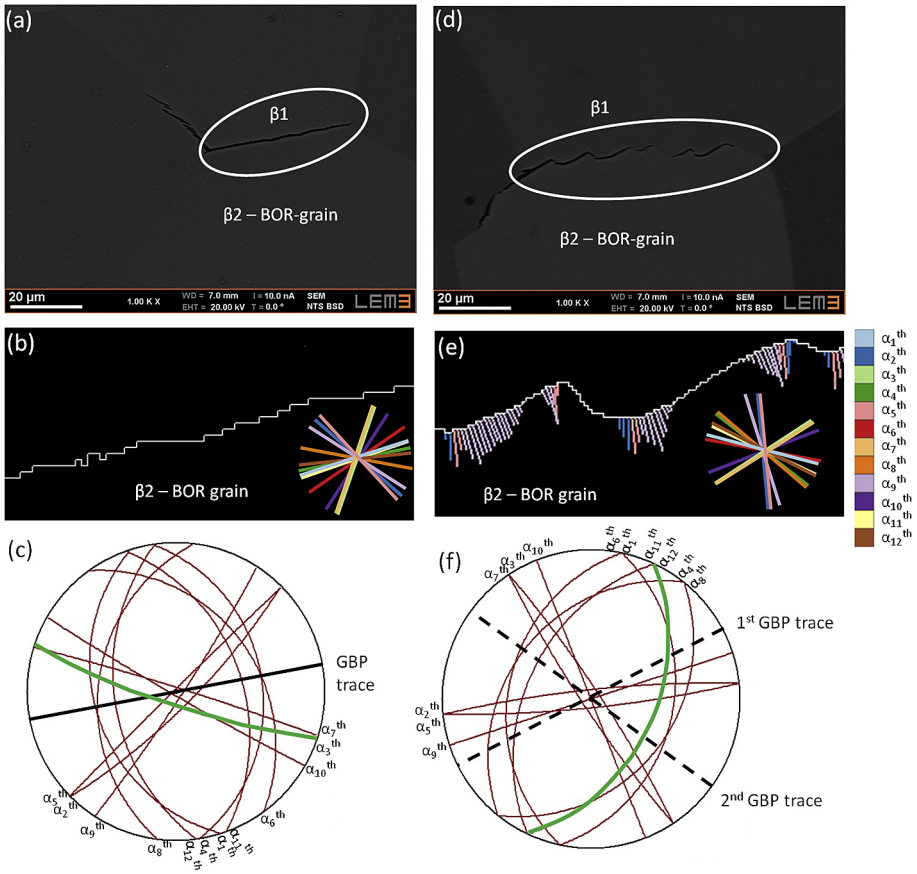

Fig. 8. Example A (planar GB) and B (zig-zag GB) showing the inconsistency between the observation and the predicted HP variants: (a,d) BSD image showing the β/α/β interface and the BOR grain, (b,e) the predicted HP variants along the GB, and (c,f) the 12 H PP and the GBP trace projected on a pole figure, the HP of the observed variant is colored in green. (For interpretation of the references to colour in this figure legend, the reader is referred to the web version of this article).

energy balance for fast boundary decoration at the early stage of transformation.

5.2. VS prediction for α_{GB} layers

An important result of our contribution gives the probability for transformed GBs to respect the double-BOR VS criterion according to the $\theta_{2\text{-BOR}}$ deviation (Fig. 7). This evolution is clarified in three steps with two characteristic $\theta_{2\text{-BOR}}$ threshold values:

(1) At GBs with $\theta_{2\text{-BOR}}$ deviation below the first threshold of 10°, the α_{GB} variant is fully predicted by the criterion. It is always

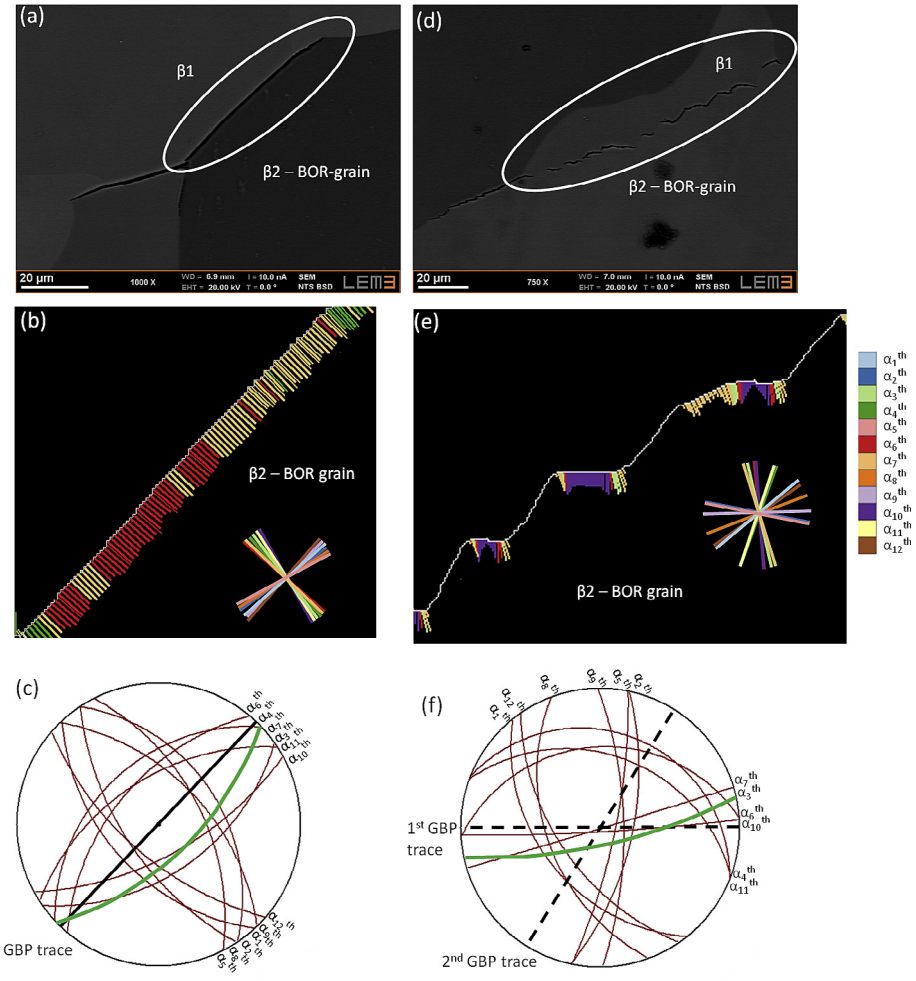

Fig. 9. Example C (planar GB) and D (zig-zag GB) showing the consistency between the observation and the predicted HP variants: (a,d) BSD image showing the β/α/β interface and the BOR grain, (b,e) the predicted HP variants along the GB, and (c,f) the 12 H PP and the GBP trace projected on a pole figure, the HP of the observed variant is colored in green. (For interpretation of the references to colour in this figure legend, the reader is referred to the web version of this article).

close to the variant pair ($\alpha_i^{th-\beta1}/\alpha_i^{th-\beta2}$) minimizing BOR with both grains. Actually it satisfies BOR with one grain (the BOR grain) and deviates more (but as less as possible) from the other (the non-BOR grain).

(2) At GBs with $\theta_{2\text{-BOR}}$ deviation increasing from 10° to the second $\theta_{2\text{-BOR}}$ threshold of 16°, a progressive drop in the double-BOR VS frequency is observed but remains higher than random occurrence.

(3) At GBs with $\theta_{2\text{-BOR}}$ deviation greater than 16°, the level of no VS (~10%) is reached (the exact value of this upper threshold should be refined on a greater dataset). The α_{GB} layer of these GBs is well aligned in BOR with one β grain but far away from the other (higher than the minimum value given by the criterion).

The double-BOR criterion was already applied in the literature on a Ti-5553 alloy for a similar GB decoration rate. The analyzed specimen was maintained for 2 h at 825 °C, corresponding to an undercooling temperature of 25 °C [6]. A larger threshold angle of 15° was claimed for 100% prediction. This is wrong on our larger data set: 3/9 GBs with $\theta_{2\text{-BOR}}$ between 10° and 16° have been found to violate the double-BOR criterion. However the data set in Ref. [6] was rather small and the large majority of analyzed GBs were in fact decorated by an α_{GB} layer satisfying double-BOR below 10° (notice that the minimum BOR deviation was not imposed). Thus the VS analysis in Ref. [6] is finally in agreement with our result and is consistent with the refined VS evolution found in the present work (Fig. 7).

One can question if the evolution of VS frequency as a function of the GB's $\theta_{2\text{-BOR}}$ deviation could be influenced by the chemical composition of the alloy, its thermo-mechanical history and the transformation conditions. For example, a higher undercooling temperature increases the driving force for nucleation and may reduce the influence of the GB character. The thermo-mechanical history may modify the GB energy distribution. Although the transformation kinetics and the inherited microtexture (at the grain level) are affected [13], no influence of the undercooling temperature on VS frequency can be evidenced by comparing published results with the present ones [6,13].

For the same alloy Ti-17 and treatment temperature (800°C), Salib et al. observed that the VS decreases as the transformation progresses (considering a $\theta_{2\text{-BOR}}$ threshold of 15°) [5]. As the GB decoration increased from 60% to 95%, the VS frequency dropped from 80% to 45% (the frequency was calculated only on the fraction of GBs able to satisfy the double-BOR condition at 15°). Our result confirms this trend: the VS frequency was of 91% at the GB decoration of 16.2% (the data are obtained with the same $\theta_{2\text{-BOR}}$ deviation of 15°). However, our findings shed a new light to interpreting

this result. Indeed, it is essential to consider the type of special GBs that are further decorated with the transformation progress (and their $\theta_{2\text{-BOR}}$ deviation) (Figs. 3 and 7). It is clear in the Ti-17 sample that strict Type II and III GBs are not numerous and are saturated at the early stage. With the transformation progress, we can assume that the 'special' GBs that further transform have a $\theta_{2\text{-BOR}}$ deviation between 10° and 16° for which the VS frequency decreases with increasing $\theta_{2\text{-BOR}}$. Moreover, when the GB decoration rate reaches 95%, most of Type I LAGBs very numerous in our sample have obviously transformed. It is likely that they have a random behavior and thus have a large implication in the drop of the VS frequency to 45%.

The implication of the HP in the VS mechanism was not relevant in our case. In fact, more than half of the 74 analyzed GBs were identified by the single trace analysis as transformed without respecting the considered HP criterion. Indeed, the trace between the $\{334\}_\beta$ HP of the selected α_{GB} layer and the GBP was always greater than 10°. The fraction of 'excluded' GBs is even higher with a smaller angle between the traces. This excludes a closeness of the selected variant HP to the GBP. This conclusion remains the same by considering the other HP near the $\{334\}_\beta$ type as often reported in the literature [16,17] (because of the large trace deviation angle of 10°). Shi performed a 3D analysis by considering the closeness of the $\{112\}_\beta$ to the GBP and concluded that such rule is frequently violated [11].

Recently, the HP VS criterion was analyzed by 3D analysis at one GB of a triple junction for a water quenched Ti-64 [10]. The HP was assumed to be of $\{55\bar{6}\}_\beta$ type (it was defined by the plane containing the lattice invariant direction $<335>_\beta$ and the $[0001]_\alpha \| <1\bar{1}0>_\beta$ direction). Pilchlak *et al* concluded that the HP of the α_{GB} variant needs to lie close (lower than 5°) to the GBP to influence the selection.

One could thus question about the fraction of GBs able to potentially respect this HP condition. We attempted to evaluate this fraction for a random poly-crystal using a Monte-Carlo simulation. First 2×10^9 GBs were generated and characterized by their 5 parameters (disorientation and GBP). Then the angle between the GBP and the closest HP of the 24 theoretical variants was computed. As a result, only 10% of the GBs have an angle below 5°. In our sample, we verified that the transformed GBs (essentially HAGBs) can be considered as randomly distributed. According to the Monte-Carlo simulation, about 10% of GBs could potentially respect the HP criteria. Thanks to the automated trace analysis, we could exclude a large majority of the 16.2% transformed GBs from the HP-criterion. The remaining transformed GBs needs to be further analyzed in 3D to ascertain the role of the HP. However, such an analysis is time consuming and need to be performed only on the GBs suspected to satisfy the criterion. The automated trace analysis with DECRYPT software is especially powerful to find relevant GB candidates.

Another VS mechanism reported in the literature but not considered in this work could be more relevant than HP-criterion. Furuhara et al. proposed that a variant may be selected if the compact direction implicated in the BOR ($<111>_\beta \| <11\bar{2}0>_\alpha$) is nearly parallel to the GBP [12]. If a trace analysis was possible for the HP criterion, it is not the case for this mechanism and the assessment would require a full 3D analysis. One should mention that this criterion is less selective because 3 distinct variants of a given β grain share a common $[111]_\beta$ direction.

5.3. Consequence for the in-service microstructure

To enhance in-service properties of Ti-alloys, it is critical to avoid (or at least hinder) as much as possible the development of large α crystallographic domains. In β-transformed microstructure, 'double α Widmanstätten colonies' growing at each side of a GB are known to be the largest ones [1]. They form from an α_{GB} precursor in BOR with both grains at special GBs. Our result shows that these special GBs form their α_{GB} layer at the early stage of transformation and thus are able to emit the first α_{WGB} double colonies. As transformation progresses and if nucleation and growth rates of additional α_{GB} layers in the same parent grains are sluggish, these colonies will be able to extend over both β grains. This contributes to the formation of large single oriented domains [5].

Our study offers to classify the criticality of a GB to develop double colonies according to the type of special GB and its double-BOR deviation. Type II and III are the most critical GBs since they form early α_{GB} layers which respect the VS criterion. Type IV GBs are second in criticality. They respect the VS criterion but the emitted double colonies at these boundaries would be smaller since their α_{GB} formation is delayed. With increasing deviation from the double-BOR condition, the VS frequency for these special HAGBs decreases. Type I GBs are lest critical because they have a delayed formation of α_{GB} and may less respect the VS criterion as discussed in the previous section.

The formation of double colonies may be avoided by tailoring the forging conditions and subsequent cooling. The distribution of prior β GBs in a material is inherited from its thermo-mechanical history and in particular its β texture and microtexture. Typical β textures encountered in Ti-alloys have been reviewed in Ref. [30]. The most commonly encountered texture in industrial product is inherited from forging (i.e. compression). It is assumed to be sharp with mixed $<111>_\beta$ and $<100>_\beta$ fibers. The GB misorientation distribution for an isotropic texture and an idealized compression texture[3] was simulated using a Monte-Carlo approach. The fraction of special GB types was quantified as a function of the $\theta_{2\text{-BOR}}$ deviation in Fig. 10. This calculation shows that a compression texture contains more special boundaries as the isotropic texture. At $\theta_{2\text{-BOR}} = 10°$, the increase is of +215% for Type I, +102% for Type III, +90% for Type IV and +48% for Type II. As a result, β forging may be optimized by taking into account the resulting β texture and microtexture as it influences the fraction of special boundaries critical for emission of large α colonies.

The second aspect that may be adjusted is the cooling after forging. In fact, it is well established that at higher undercooling the transformation kinetics is accelerated by either a more rapid nucleation and growth kinetics of α_{GB} layers allowing the simultaneous growth of several colonies or by the nucleation of α platelets on intragranular nucleation sites [31]. The formation of large double colonies could thus be limited or avoided by a more efficient cooling rate favoring a rapid nucleation and growth on most HAGBs followed by the growth of numerous colonies and/or by the nucleation and growth of intragranular α platelets. The possibility to control the effect of the cooling rate, in particular in large parts, will strongly depend on the chemical composition of the alloy, its quenchability and the thermo-mechanical treatment before the cooling.

6. Conclusions

This contribution offers a deep analysis of early GB decoration in a β-metastable titanium alloy (1) to identify the probability of a GB to transform early according to a disorientation criterion and (2) to predict the orientation of the α_{GB} layers.

[3] 50%<111> + 50%<100>. For each fiber a noise was added by rotating the ideal fiber orientation around an axis perpendicular to the fiber axis of an amplitude following a Gaussian distribution of 20° at half width.

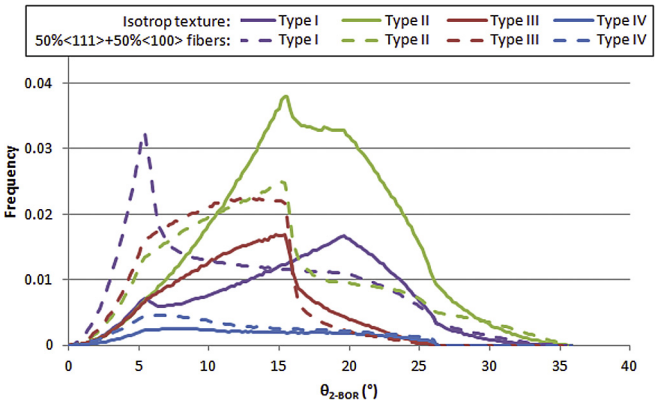

Fig. 10. Frequency of special GB types as a function of $\theta_{2\text{-BOR}}$ deviation for two textures (isotropic and fiber like).

(1) Our result confirms that the α_{GB} layers precipitate on HAGBs with a much higher frequency than on LAGBs at the early stage of transformation. The major finding is the important differences in transformation frequency observed according to the type of special GBs (a GB is called special if it is able to form an α_{GB} layer satisfying BOR with both grains within an angular deviation $\theta_{2\text{-BOR}}$). We found that special HAGBs disoriented close to 49.5°, 60°/<110> have a transformation frequency close to 100%. Their transformation frequency decreases with increasing $\theta_{2\text{-BOR}}$ deviations but remains higher than for general HAGBs up to $\theta_{2\text{-BOR}} = 10°$. Unexpectedly, special GBs disorientated by 60°/<111> have no advantage for fast transformation. The special LAGBs disorientated by 10.5°/<110> do not transform early despite their high amount in our sample. As special GBs (49.5°, 60°/<110>) were rare in our sample, the major fraction of early transformed boundaries were actually general HAGBs.

(2) The α_{GB} layers observed at special GBs (up to $\theta_{2\text{-BOR}} = 10°$) always minimizes BOR with both grains (respecting the so-called double-BOR VS criterion). Beyond $\theta_{2\text{-BOR}} = 10°$, a progressive drop in VS frequency is observed. When $\theta_{2\text{-BOR}} > 16°$, it reaches the level of no VS (~10%). The evolution of the VS frequency with the $\theta_{2\text{-BOR}}$ deviation is essential to predict the occurrence of this mechanism according to a given β microtexture and the transformation progress. It explains the main differences reported in the literature. From this research, it is possible to evaluate the frequency of critical α_{GB} precursors according to the β microtexture and phase transformation path.

In addition the relevance of the HP∥GBP criterion is also discussed. This criterion consists in selecting the variant with the closest HP to the GBP. The single trace analysis performed in this contribution excludes this criterion for the majority of analyzed α_{GB} layers.

Finally, one has to point out the statistics behind our conclusions: more than 1000 GBs were analyzed by EBSD. This enables the reliable VS frequency to distinguish the effective occurrence of a mechanism from its random occurrence. Our home-made software 'DECRYPT' is a key tool to obtain the statistical data in this framework.

Acknowledgements

This work was supported by the French State through the program "Investment in the future".operated by the National Research Agency (ANR) and referenced by ANR-11-LABX-0008-01 (LabEx DAMAS).

References

[1] R. Whittaker, K. Fox, A. Walker, Texture variations in titanium alloys for aeroengine applications, Mater. Sci. Technol. 26 (2010) 676–684.
[2] G. Lutjering, Influence of processing on microstructure and mechanical properties of (α+β) titanium alloys, Mater Sci. Eng. A 243 (1998) 32–45.
[3] G.R. Yoder, F.H. Froes, D. Eylon, Effect of microstructure, strength, and oxygen content on fatigue crack growth rate of Ti-4.5AI-5.0Mo-1.5Cr (CORONA 5), Metall. Trans. A 15 (1984) 183–197.
[4] W.H. Miller, R.T. Chen, E.A. Starke, Microstructure, creep, and tensile deformation in Ti-6Al-2Nb-1Ta-0.8Mo, Metall. Trans. A 18 (1987) 1451–1468.
[5] M. Salib, J. Teixeira, L. Germain, E. Lamielle, N. Gey, E. Aeby-Gautier, Influence of transformation temperature on microtexture formation associated with α precipitation at β grain boundaries in a β metastable titanium alloy, Acta Mater. 61 (2013) 3758–3768.
[6] R. Shi, V. Dixit, H.L. Fraser, Y. Wang, Variant selection of grain boundary α by special prior β grain boundaries in titanium alloys, Acta Mater. 75 (2014) 156–166.
[7] N. Stanford, P.S. Bate, Crystallographic variant selection in Ti-6Al-4V, Acta Mater. 52 (2004) 5215–5224.
[8] S.M.C. van Bohemen, A. Kamp, R.H. Petrov, L.A.I. Kestens, J. Sietsma, Nucleation and variant selection of secondary α plates in a β Ti alloy, Acta Mater. 56 (2008) 5907–5914.
[9] G.C. Obasi, S. Birosca, D.G. Leo Prakash, J. Quinta da Fonseca, M. Preuss, The influence of rolling temperature on texture evolution and variant selection during α→β→α phase transformation in Ti-6Al-4V, Acta Mater. 60 (2012) 6013–6024.
[10] A.L. Pilchak, D. Banerjee, J.C. Williams, Grain boundary α and β grain boundary orientation in titanium alloys, in: V. Venkatesh, A.L. Pilchak, J.E. Allison, S. Ankem, R. Boyer, J. Christodoulou, H.L. Fraser, M.A. Imam, Y. Kosaka, H.J. Rack, A. Chatterjee, A. Woodfield (Eds.), Ti-2015, Wiley online library, 2015, pp. 425–430.
[11] R. Shi, V. Dixit, G.B. Viswanathan, H.L. Fraser, Y. Wang, Experimental assessment of variant selection rules for grain boundary α in titanium alloys, Acta Mater. 102 (2016) 197–211.
[12] T. Furuhara, S. Takagi, H. Watanabe, T. Maki, Crystallography of grain boundary α precipitates in a β titanium alloy, Metall. Trans. A 27 (1996) 1635–1646.
[13] M. Salib, J. Teixeira, L. Germain, B. Denand, N. Gey, E. Aeby-Gautier Williams, Influence of α precipitation at β/β grain boundaries on a Microtexture in A β-metastable titanium alloy with and without previous deformation, in: V. Venkatesh, A.L. Pilchak, J.E. Allison, S. Ankem, R. Boyer, J. Christodoulou, H.L. Fraser, M.A. Imam, Y. Kosaka, H.J. Rack, A. Chatterjee, A. Woodfield (Eds.), Ti-2015, Wiley online library, 2015, pp. 405–414.
[14] L. Germain, N. Gey, M. Humbert, Reliability of reconstructed beta-orientation maps in titanium alloys, Ultramicroscopy 107 (2007) 1129–1135.
[15] Y.C. Liu, Martensitic transformation in binary Ti-alloys, Trans. AIME 206 (1956) 1036–1040.
[16] T. Furuhara, T. Ogawa, T. Maki, Atomic structure of interphase boundary of an a precipitate plate in a β Ti-Cr alloy, Philos. Mag. 72 (1995) 175–183.
[17] F. Ye, W.Z. Zhang, D. Qiu, A TEM study of the habit plane structure of intragrainular proeutectoid α precipitates in a Ti–7.26 wt%Cr alloy, Acta Mater. 52 (2004) 2449–2460.
[18] A. Settefrati, B. Appolaire, E. Aeby-Gautier, Y. Le Bouar, G. Khelifati, Effect of oxygen content and working on microstructural evolution and mechanical properties of biomedical Ti-6Al-4V alloy wire, in: L. Zhou, H. Chang, Y. Lu, D. Xu (Eds.), Ti-2011, Science Press Beijing, Beijing, 2012, pp. 473–476.
[19] M. Cottura, B. Appolaire, A. Finel, Y. Le Bouar, Phase field study of acicular growth: role of elasticity in Widmanstätten structure, Acta Mater 72 (2014) 200–210.
[20] A. Settefrati, Étude expérimentale et modélisation par champ de phase de la formation de α dans les alliages de titane β-métastable, PhD Thesis, Université de Lorraine, Nancy, 2012.
[21] R. Shi, N. Ma, Y. Wang, Predicting equilibrium shape of precipitates as function of coherency state, Acta Mater. 60 (2012) 4172–4184.
[22] J.K. Mackenzie, Second paper on statistics associated with the random disorientation of cubes, Biometrika 45 (1958) 229–240.
[23] J. Teixeira, B. Appolaire, E. Aeby-Gautier, S. Denis, G. Cailletaud, N. Späth, Transformation kinetics and microstructures of Ti17 titanium alloy during continuous cooling, Mater Sci. Eng. A 448 (2007) 135–145.
[24] M. Salib, Étude cinétique et cristallographique de la précipitation de la phase α aux joints de grains β/β dans un alliage de titane, PhD thesis, Université de Lorraine, Nancy, 2015.
[25] E.J. Lieberman, A.D. Rollett, R.A. Lebensohn, E.M. Kober, Calculation of grain boundary normals directly from 3D microstructure images, Model. Simul. Mater Sci. Eng. 23 (2015), 035005.
[26] H. Sharma, S.M.C. van Bohemen, R.H. Petrov, J. Sietsma, Three-dimensional analysis of microstructures in titanium, Acta Mater. 58 (2010) 2399–2407.
[27] A. Morawiec, PAN software, 2016. http://imim.pl/personal/adam.morawiec/A_Morawiec_Web_Page/downloads.html.

[28] J. Teixeira, L. Germain, E. Lamielle, N. Gey, E. Aeby-Gautier, B. Appolaire, Microstructure and microtexture associated to heterogeneous precipitation of the a phase on β/β boundaries in Ti17 alloy:Influence of first stages of αGB formation, in: L. Zhou, H. Chang, Y. Lu, D. Xu (Eds.), Ti-2011, Science Press Beijing, Beijing, 2012, pp. 464–467.
[29] S. Ratanaphan, D.L. Olmsted, V.V. Bulatov, E.A. Holm, A.D. Rollett, G.S. Rohrer, Grain boundary energies in body-centered cubic metals, Acta Mater. 88 (2015) 346–354.
[30] A.K. Singh, R.A. Schwarzer, Evolution of texture during thermomechanical processing of titanium and its alloys, Trans. Indian Inst. Met. 61 (2012) 371–387.
[31] E. Aeby-Gautier, F. Bruneseaux, J. Da Costa Teixeira, B. Appolaire, G. Geandier, S. Denis, Microstructural formation in Ti alloys: in-situ characterization of phase transformation kinetics, JOM 59 (2007) 54–58.